

# Airborne Snow Concentration and Visibility

J. R. Stallabrass, National Research Council of Canada

Little information is available on the probability distribution of the mass concentration of snow in the atmosphere. Such a deficiency became apparent as the result of engine malfunctions in helicopters while flying in falling snow. To help rectify this deficiency and so provide data for the meaningful design and testing of aircraft engine intake systems for operation in snow, a program was initiated to measure the snow mass content of the air. In conjunction with the measurements of snow concentration various other meteorological parameters were measured. It was found that the snow concentration may be estimated from the visibility with reasonable accuracy, thus offering the hope that concentration statistics may be derived for any location where climatological data on visibility are available. This is currently being tested using climatological data for Ottawa.

Other papers in this Symposium deal with problems or investigations of snow either on the ground or within a metre or so above it, i.e. blowing snow. This paper addresses itself to the mass concentration of snow in the atmosphere at greater heights and in the absence of blowing snow, although it is likely that the demonstrated relationship between mass concentration and visibility should apply equally to blowing snow as to falling snow.

Little interest in a detailed knowledge of the mass concentration of snow in the atmosphere was evinced until a few years ago when certain helicopters were found to develop engine malfunctions when flying in snow (1). Until then, aircraft flight through snow had presented few problems because the dry snow crystals did not adhere to the surfaces on which they impinged; however, the helicopters in question had rather sinuous engine intakes where snow accumulations could occur, particularly where stray heat warmed the intake wall. The subsequent release of these snow accumulations frequently resulted in engine flameout and, in a few instances, in serious crashes. It was evident that in order to permit the meaningful design and qualification testing of aircraft engine intake systems, a quantitative knowledge of the snow mass concentration in the air was needed.

A knowledge of the snow concentration also has applications where it is necessary to know the snow mass flux under circumstances where the horizontal component of the flux is significant relative to the vertical flux (precipitation rate), whether that horizontal flux is due to movement of an object (such as a surface vehicle or aircraft), the induction of air and snow into an air intake system (such as that of a stationary gas turbine installation), or as a result of wind action (such as the accumulation of wet snow on transmission lines or communication antennae).

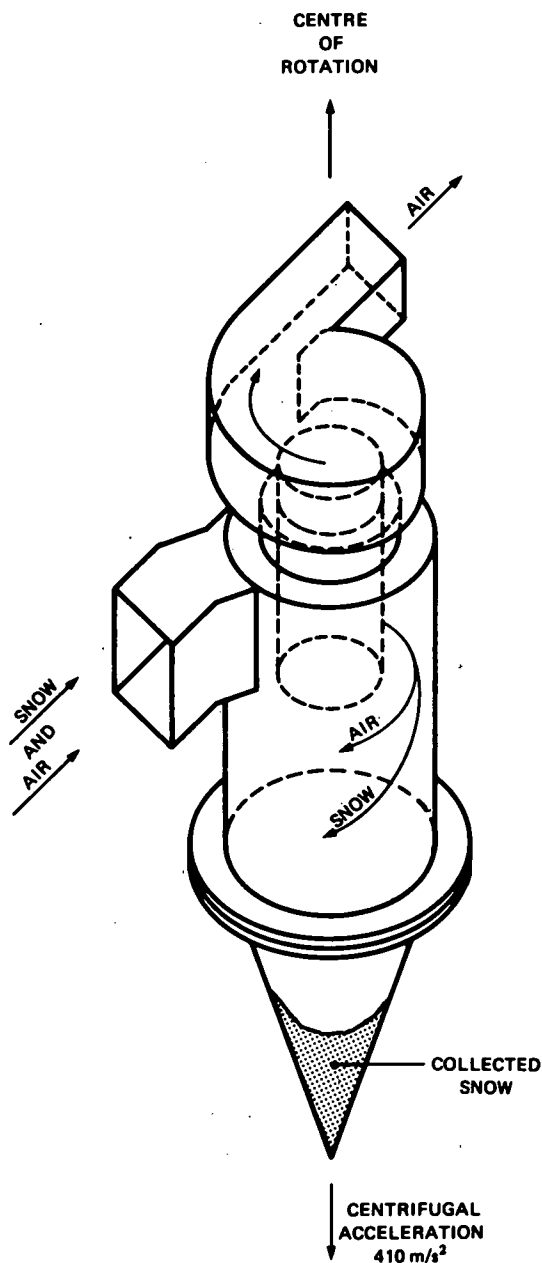
In theory, the snow mass concentration can be derived from the precipitation rate, but to do this a knowledge of the fall velocities of the spectrum of snow particles comprising the snowfall is required. Since these may vary by as much as an order of magnitude depending on snow crystal size and type (2,3,4), it is clear that a detailed knowledge of the characteristics of the particular snowfall would be required. Add to this the uncertainty of measurement of snow precipitation rate, particularly under conditions of even moderate winds, and also the fact that precipitation rates are usually reported as, at best, one-hour, and more usually, six-hour averages, it is clear that the use of precipitation rate to derive mass concentration statistics for snow is rather marginal.

In present weather observing practice, snow intensity is normally defined in a very qualitative way in terms of visibility, thus providing no indication of mass concentration. Thus it was concluded that an independent and direct means of measuring snow mass concentration was required to derive reliable concentration probabilities. Further, it was felt that if a correlation could be found to exist between the measured concentration and some routinely measured meteorological parameters, either alone or in combination, the prevailing snow concentration could be derived without resort to specialized measuring equipment, and concentration probabilities could be derived for any locality where meteorological records were available.

## Methods of Measurements

The basic approach used to measure snow concentration was to sample a known volume of the atmos-

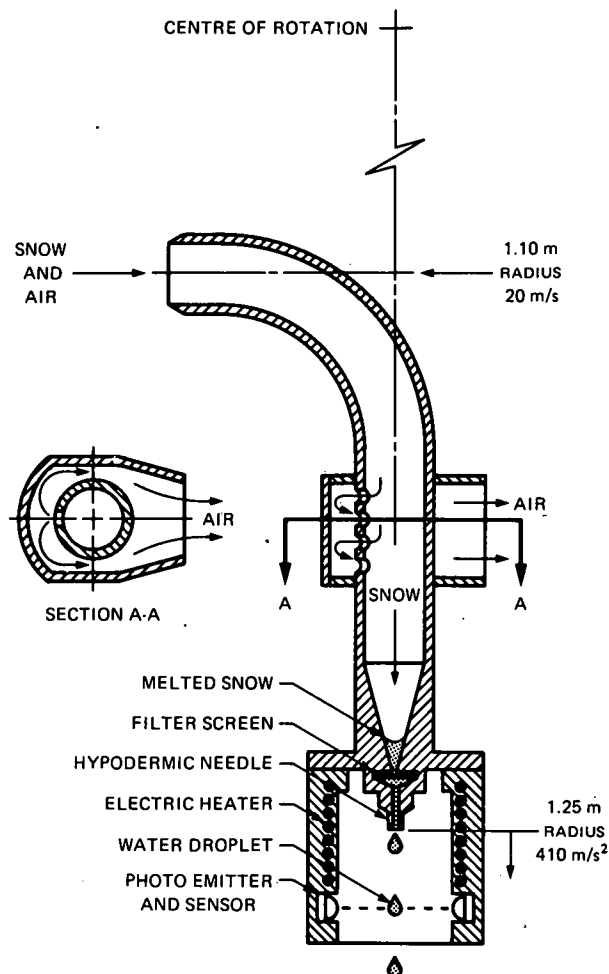
Figure 1. Cyclone separator used for manual measurement of snow mass concentration.



phere and to separate from it the snow for measurement of its mass. The apparatus consisted of a sampling device mounted at the end of an arm rotating in a horizontal plane at sufficient height above the surrounding surface as to be unaffected by blowing snow.

The type of sampling device used for the bulk of the data was a cyclone separator (Figure 1) mounted with its axis aligned with the radial arm. Flow through the device ensured high catch efficiency while both cyclone and centrifugal action ensured efficient separation of the snow from the air with little chance of particle re-entrainment in the exhausting air. The separated snow was retained in the device and weighed after a given collection period (in the order of 2 to 6 minutes depending largely on intensity), so giving a measure of the average concentration during that period.

Figure 2. Automatic sampler used for snow mass concentration measurement.



In addition an automatic snow sampler has been under development and was put into use for the first time in early 1977 for evaluation against the cyclone device. Mounted on the opposite arm to the cyclone, it collects snow in a simplified form of inertial separator (Figure 2). The collected snow is melted and allowed to flow through a hypodermic needle under the influence of the centrifugal acceleration. The resulting droplet stream is monitored photoelectrically and the pulses so generated are counted over a given time period ( $\sim 1$  minute) to obtain the snow concentration. Using the drop size data of Harkins and Brown (5), the resulting performance was found to be in close agreement with the concentration measurements provided by the cyclone device.

Simultaneously with the snow concentration measurements the following associated measurements were made adjacent to the snow sampling site:

1. Air temperature.
2. Dew point.
3. Wind speed and direction.
4. Observed visibility.
5. Precipitation rate.
6. Output of a Videograph back-scatter visibility meter.
7. Snow crystal type and estimate of size.

Table 1. Snow type categories.

Type Category	Designation	Description	Magono and Lee Classification
1	P	Plates and Broad Branched Crystals	Pl <sub>a</sub> , Pl <sub>b</sub> , Pl <sub>c</sub> , P7 <sub>a</sub>
2	D	Dendritic and Stellar Crystals	Pl <sub>d</sub> , Pl <sub>e</sub> , Pl <sub>f</sub> , P2 <sub>a</sub> , P2 <sub>b</sub> , P2 <sub>c</sub> , P2 <sub>d</sub> , P7 <sub>b</sub> , CP1 <sub>b</sub>
3	RD	Rimed Plates and Dendrites	R1 <sub>c</sub> , R1 <sub>d</sub> , R2 <sub>a</sub> , R2 <sub>b</sub> , R3 <sub>a</sub>
4	G	Graupel	R3 <sub>b</sub> , R3 <sub>c</sub> , R4 <sub>a</sub> , R4 <sub>b</sub> , R4 <sub>c</sub>
5	N	Needles, etc.	N1 <sub>a</sub> , N1 <sub>b</sub> , N1 <sub>c</sub> , N1 <sub>d</sub> , N1 <sub>e</sub> , N2 <sub>a</sub> , N2 <sub>b</sub> , N2 <sub>c</sub>
6	RN	Rimed Needles	R1 <sub>a</sub> , R1 <sub>b</sub>
7	C	Columns, Bullets, etc.	C1 <sub>b</sub> , C1 <sub>c</sub> , C1 <sub>d</sub> , C1 <sub>e</sub> , C1 <sub>f</sub> , C2 <sub>a</sub> , C2 <sub>b</sub> , CP1 <sub>a</sub> , CP2 <sub>a</sub>
8	S	Multiple Capped Columns, Side Plane Assemblages, etc.	CP1 <sub>c</sub> , S1, S2, S3
9	I	Miscellaneous, including Broken Crystals, etc.	I1, I2, I3 <sub>a</sub> , I3 <sub>b</sub> , I4

Items 1, 2, 3, 5 and 6 above were recorded on a digital data acquisition system at discrete intervals. The sampling interval was normally one minute when manual snow concentration measurements were being made, and 10 minutes during automatic operation.

The reference points for the observed visibility estimates were mostly tall buildings lying largely in the quadrant between west and south from the sampling site. This directionality may have contributed some scatter or bias to any relationships involving visibility whenever the snow intensity was variable.

The heated precipitation gauge used proved unreliable in its original form, but now, after considerable modification, consistent operation has been achieved. This instrument provides a signal for each 0.2 mm of water collected.

Snow crystal type was observed by allowing a number of crystals or flakes to fall onto a velvet covered board. The snow crystal classification scheme of Magono and Lee (6) was used in recording crystal type. However, for the purposes of correlating the data, many of these types were grouped together reducing the number of individual categories to 9, as shown in Table 1. In most cases a variety of crystal types co-existed, but one type usually predominated; the snowfall was then categorized according to the predominant type. Where it was impossible to assign a predominant type, the sample was included in the miscellaneous (I) type.

#### Relationship between Concentration and Visibility

Multiple regression analysis techniques were applied to the snow concentration and the other measured quantities, but apart from a highly significant correlation between concentration and visibility (and Videograph reading), no other significant influences were discernible. It was thought that, since the basic visibility (in the absence of snow) was dependent to a large extent on relative humidity, the introduction of this parameter into regression would help to resolve some of the scatter of data points, particularly in the low concentration/high visibility region which can be most affected by the effects of haze. However, it was found that the relative humidity was itself influenced by the concentration and hence was not an independent variable that could properly be taken into regression.

Except for some cases of very small ice crystals (<0.5 mm) no systematic effect due to crystal size was discernible. It is likely that any effect due to size was masked by variations in crystal form and by uncertainties in measurement, particularly those due to directional and time variations in concentration and visibility during the sample.

Physical reasoning suggests that the relation between snow concentration and visibility should conform to a log-log relationship, the coefficient in which should be about -1.33. Figure 3, which shows all the points measured by the manual snow

Figure 3. Data plot of manual snow mass concentration measurements against observed visibility for all snow types, and showing regression line  $\log_{10} C = 3.315 - 1.286 \log_{10} V$ . 832 Data points.

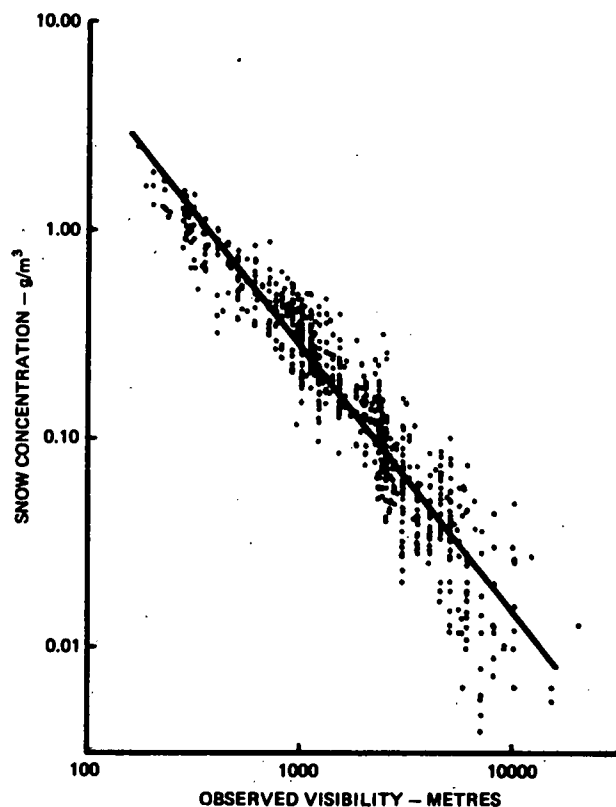


Table 2. Regression results,  $\log_{10}$  concentration vs  $\log_{10}$  visibility, for various snow types and groups of types.

Snow Types	No. of Samples	Regression Equation	Correlation Coefficient	Std. Error of Estimate
All	832	$\log_{10}C = 3.315 - 1.286 \log_{10}V$	-0.943	0.174
1,7 & 8	312	$\log_{10}C = 3.579 - 1.367 \log_{10}V$	-0.954	0.130
3,4 & 6	310	$\log_{10}C = 3.069 - 1.202 \log_{10}V$	-0.949	0.173
2	77	$\log_{10}C = 4.130 - 1.564 \log_{10}V$	-0.930	0.171
5	6	$\log_{10}C = 2.292 - 1.022 \log_{10}V$	-0.972	0.114
9	127	$\log_{10}C = 3.258 - 1.264 \log_{10}V$	-0.930	0.209

sampler over a period of seven winters, indicates that the regression equation

$$\log_{10}C = 3.315 - 1.286 \log_{10}V$$

or  $C = 2100 V^{-1.29}$

(where the mass concentration  $C$  is in  $g/m^3$  and the visibility  $V$  is in metres) does in fact represent the measured data reasonably well, but with some slight overestimation at low concentrations where the effects of haze become more predominant.

In general it was found that individual snow types gave better correlation and/or lower standard error of the estimate than when all the data for all snow types was consolidated. Some of the individual snow types had similar regression equations and could be grouped together with little effect on the regression statistics. Hence types 1, 7 and 8 (i.e. plates and broad branched crystals, columns and bullets, and side plane assemblages, etc.) could be treated together as a group, and so could all the rimed types (i.e. types 3, 4 and 6). The regression equations for these two groups and for the remaining individual snow types are shown in Table 2.

It is clear from these results that the differing light scattering characteristics of different snow crystal types do, as expected, have an effect on the visibility. However, other modifying influences, which are difficult to identify or isolate, appear to be as significant as the crystal form in causing variation in the observed visibility for a given snow mass concentration. Such influences may include the crystal size distribution in the snow-fall or the presence of other crystal types along with the predominant type. In none of the correlations was there any marked indication that the aggregation of individual snow crystals into snowflakes had any consistent effect, although it is possible that the generally poorer correlation exhibited by the stellar and dendritic/type crystals (the type most commonly forming flakes) may have resulted in part from this cause.

A marked difference in the concentration-visibility relationship between unrimed and rimed snow of the same type (i.e. types 2 and 3) was evident. Two factors are probably operative, the added mass relative to the crystal dimensions resulting from the accreted rime, and the modification of the basic hexagonal form of the crystal and the resulting effect on scattering characteristics. In spite of this, the degree of riming (i.e. from snow crystals with a few frozen droplets to graupel) did not appear to have any consistent effect.

#### Relation between Concentration and Videograph Output

The Videograph backscatter meter measures the amount of light scattered from a projector beam back into a photosensitive receiver placed alongside the projector. The amount of scattered light entering the receiver depends on the number and nature of the light scattering elements in the beam. Thus the possibility existed that the instrument would prove useful in providing a measure of the mass concentration of snow in the atmosphere. Accordingly mean values of the Videograph output current were recorded for all snow concentration samplings. Various functional relationships between the measured snow concentration and the Videograph output were attempted in regression analysis, and the one found to give the highest correlation coefficient and the lowest standard error of the estimate was found to be a log-log relationship.

Two Videograph instruments have been used at different times during these measurements; the first one was of a batch built for the Canadian Coast Guard as a fog warning device, while the one that has been in use for the last two winters is of more recent manufacture and has the same intrinsic calibration as instruments supplied to the Canadian Atmospheric Environment Service for visibility measurement at remote automatic meteorological stations. Since the calibrations of the two instruments differ slightly, only the data taken with the latter instrument is presented here. This data is shown in Figure 4, and its regression equation was found to be

$$\log_{10}C = 0.143 + 4.648 \log_{10}I_V$$

or  $C = 1.39 I_V^{4.65}$

(where the mass concentration  $C$  is in  $g/m^3$  and the Videograph output current  $I_V$  is in mA).

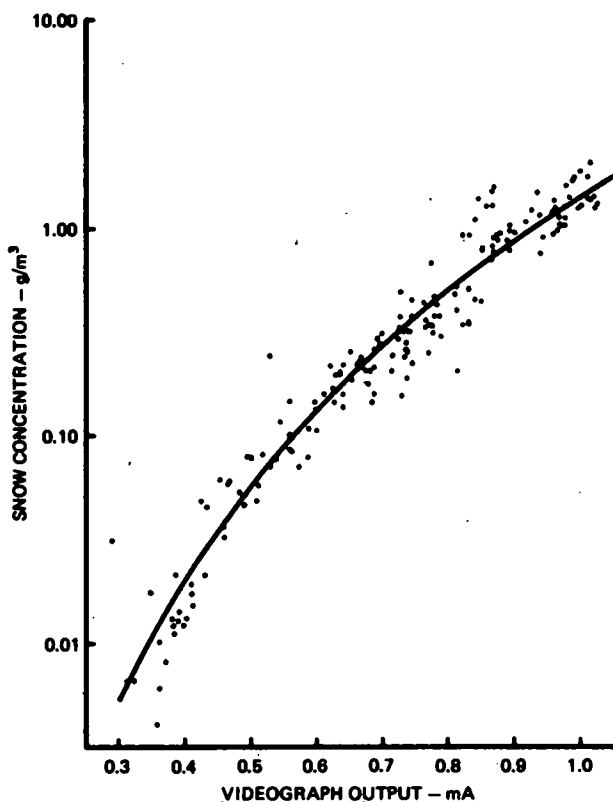
Like the visibility results, rather better correlation is obtained by considering individual snow types; however, less differentiation between the various types was observed, so that all the unrimed types with the exception of type 1 (i.e. plates) could be treated as one group (no observation of type 5, unrimed needles, was made in the last two winters), while the rimed types (3, 4 & 6) formed another group. The regression results for these two groups and for type 1 snow are presented in Table 3.

The regression results for the unrimed group (i.e. types 2, 7, 8 and 9) differed little from that for all the snow types combined. However, type 1 snow (hexagonal plates) exhibited a lower Videograph output for a given mass concentration than other types, while the rimed types gave a slightly higher output. Both type 1 and the rimed snow group showed extremely good correlation.

Table 3. Regression results,  $\log_{10}$  concentration vs  $\log_{10}$  Videograph output current, for various snow types and groups of types.

Snow Types	No. of Samples	Regression Equation	Correlation Coefficient	Std. Error of Estimate
All	176	$\log_{10} C = 0.143 + 4.648 \log_{10} I_V$	0.970	0.154
1	17	$\log_{10} C = 0.347 + 4.880 \log_{10} I_V$	0.982	0.059
2,7,8 & 9	94	$\log_{10} C = 0.152 + 4.614 \log_{10} I_V$	0.968	0.153
3,4 & 6	65	$\log_{10} C = 0.093 + 4.773 \log_{10} I_V$	0.988	0.110

Figure 4. Data plot of manual snow mass concentration measurements against Videograph output current for all snow types, and showing regression line  $\log_{10} C = 0.143 + 4.648 \log_{10} I_V$ . 176 Data points.



Liou (7) suggests that back-scattering from randomly oriented ice needles and columns is small, while plates and irregular types of crystals have strong backscattering returns. However, these results indicate that plates have a smaller backscatter than the other snow types. This is undoubtedly because plates tend to fall flat rather than with random orientation, so that only their edges are presented to the Videograph beam, thus resulting in low backscatter relative to their overall size. Rimed crystals, conversely, give a larger backscatter than their unrimed counterparts, probably because orientation effects are less critical.

Rather less scatter is evident in the Videograph results at low snow concentrations than is the case with observed visibility (c.f. Figures 3 and 4). This would seem to be because the Videograph senses the backscatter from the near field only, and is therefore not so sensitive to the

effects that haze has on visibility when longer visual paths are involved.

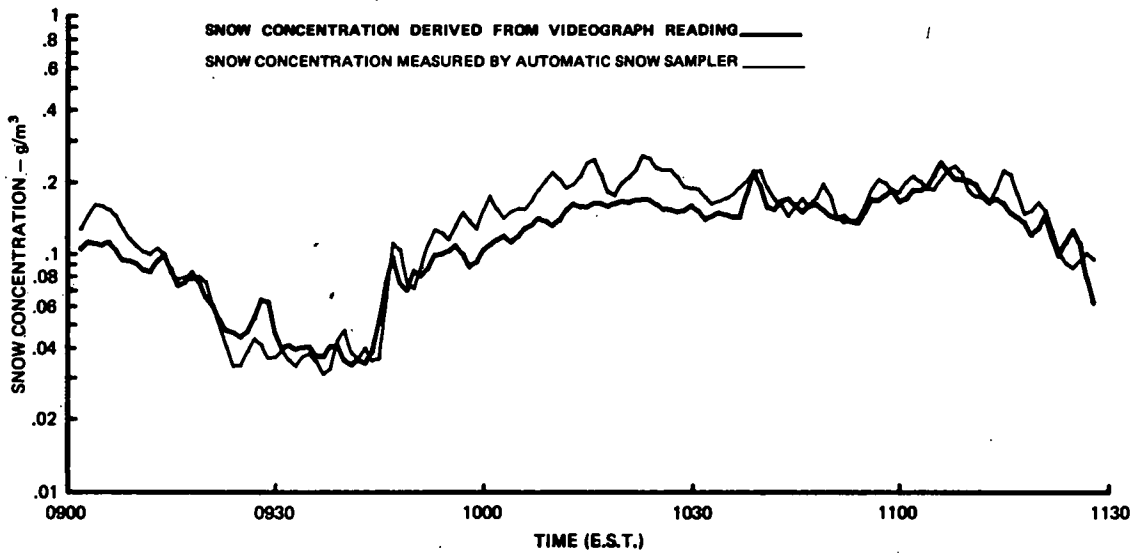
It is evident from these results that a backscatter visibility meter is a useful device for estimating snow concentration. This is demonstrated further by Figures 5 and 6 which compare the snow concentration as deduced from the Videograph output with that measured by the automatic snow sampler. Figure 5 shows a 2½-hour segment of a snowstorm during which samplings were made each minute. A three-point smoothing has been applied to this data since the Videograph readings were instantaneous values, while the snow sampler readings were the average snow concentration over a 50-second period between Videograph samples. Figure 6 shows the complete history of a snowstorm of 16 hours duration. In this case samplings were made every 10 minutes, the automatic snow sampler readings being the 50-second average immediately following the instantaneous Videograph reading. This data is unsmoothed. Both examples show good prediction by the Videograph of the snow mass concentration, with predicted values lying within approximately a factor of 2 of the measured concentration.

#### Relation between Concentration and Air Temperature

In Figure 7 the temperature dependence of the mass concentration is shown in the form of a scatter plot, using only data from the manual snow sampler. Until last winter, no discernible relationship between maximum snow concentration and surface air temperature was evident; however, some extremely high concentrations at temperatures between  $-2^{\circ}\text{C}$  and  $-4^{\circ}\text{C}$  that were recorded last winter now suggest an increasing mass concentration with increasing surface temperature. Such a relationship is perhaps not entirely to be expected since the temperature at ground level may bear little relationship to that at those levels at which formation and growth of the snow crystals took place. The great variation of crystal types falling concurrently on many occasions, the frequent complex crystal forms, and the occurrence of riming all attest to the variations in temperature and saturation of the air encountered by the snow particles during their lifetime.

Figure 7 suggests that there is perhaps a bimodal relationship between maximum concentration and temperature, with maxima at about  $-12^{\circ}\text{C}$  and  $-3^{\circ}\text{C}$ . The snow types contributing to the peak at about  $-12^{\circ}\text{C}$  were rimed dendrites, rimed needles and miscellaneous rimed particles, while those responsible for the mode at about  $-3^{\circ}\text{C}$  were plates, rimed dendrites, graupel, miscellaneous rimed particles, and to a lesser degree, side plane assemblages. The peak values at both peaks occurred with snow particles that could not be uniquely typed and

Figure 5. Comparison between snow mass concentration derived from Videograph output and that measured by automatic snow sampler. Portion of storm of 22 February 1977 sampled at 1-minute intervals.



hence were included in the miscellaneous category, although in both cases the particles were rimed. The total number of observations in each temperature range suggest that the frequency of occurrence of snow events increases with temperature up to a maximum in the temperature range of  $-2^{\circ}\text{C}$  to  $-4^{\circ}\text{C}$ . Over one half of the observations (and hence, we may assume, over one half of the time that snow occurs) are within the temperature range  $0$  to  $-8^{\circ}\text{C}$ .

#### Probability Distribution of Snow Concentration

The cumulative distribution curve of 758 discrete snow concentration measurements made over a period of six winters is shown as curve (a) in Figure 8. This curve shows that the mean of the measurements was about  $0.15 \text{ g/m}^3$ , while a concentration of  $1.0 \text{ g/m}^3$  was exceeded by about 5% of the

measurements.

It had been hoped that these measurements might represent a reasonably random sampling of all snow events during this period; however, it must be conceded that the frequency of sampling during heavy snowfalls tended to be greater than during lighter, less significant events. Thus it may be assumed that curve (a) is biased to heavier concentrations than those of a true random distribution.

The correlation that has been shown to exist between snow concentration and visibility provides another tool for deriving probability distributions of snow concentration at any location for which climatological records are available. The probability distribution has been derived in this way for Ottawa by converting to equivalent snow concentration the hourly visibility readings during reported snowfall for the 20-year period 1955-1974. This is shown as curve (b) in Figure 8. All obser-

Figure 6. Comparison between snow mass concentration derived from Videograph output and that measured by automatic snow sampler. Storm of 20-21 January 1978 sampled at 10-minute intervals.

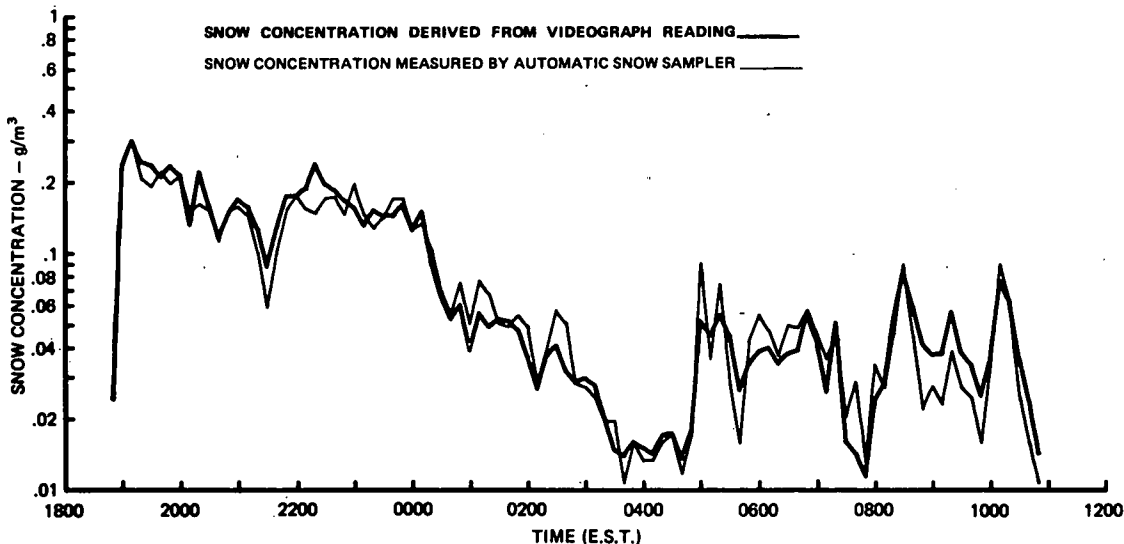
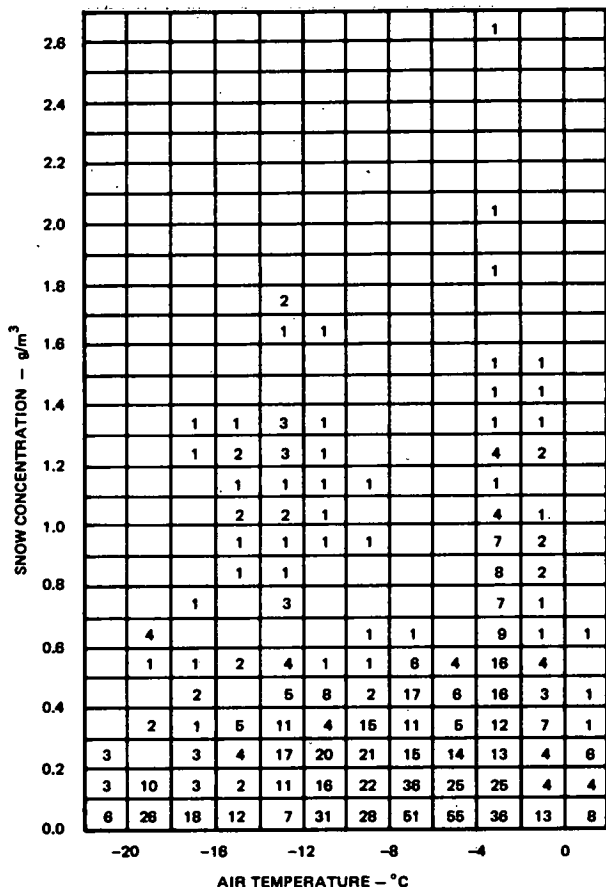


Figure 7. Plot showing number of observations within a given interval ( $0.1 \text{ g/m}^3$ ) of snow concentration for each  $2^\circ\text{C}$  interval of air temperature. Total number of observations = 851.



variations of greater than 8 km were grouped into one sample class, so that a tentative continuation of the curve to higher visibilities is shown as a broken line in the figure. Clearly a considerable discrepancy exists between the two curves.

With the introduction of the automatic snow sampler into service, performing a sample every ten minutes during all snowfall events, another means of verifying the probability distribution has become available. To date only five storms have been fully analysed, and, although they hardly comprise a representative sample, their concentration distribution is nevertheless presented as curve (c) in Figure 8. This seems to reinforce the belief that curve (a) overestimates the frequency of higher concentrations, while at the same time suggesting that curve (b) might overestimate the frequency of lower concentrations. Only continued data from the automatic sampler over a number of winters will resolve this and decide the usefulness of climatological visibility data for deriving the snow concentration distribution.

#### General Observations

The maximum snow concentration measured during this work was  $2.66 \text{ g/m}^3$  which was an average value over a 3-minute sampling period. Three snow crystal types were identified but no one was judged predominant so the sample was classed in the Miscellaneous category. The three snow types were rimed columns

(R1b), densely rimed stellar crystals (R2b), and rimed broken branches (I3b). Crystal sizes were about 2 to 3 mm with some aggregates of about 5 mm. Visibility at this concentration was 170 metres and the temperature  $-2.5^\circ\text{C}$ .

The second peak value, occurring at  $-12.7^\circ\text{C}$ , was  $1.73 \text{ g/m}^3$  and was a 4-minute average value. This sample was also placed in the Miscellaneous category, but comprised rimed needles (R1a), densely rimed plates (R2a), and multiple capped columns (CPlc). Crystal sizes were about 2 to 3 mm but with no aggregation into flakes. Visibility was 200 metres. It is of interest to note that on this occasion the mass concentration continuously exceeded a value of  $1 \text{ g/m}^3$  for a period of 1.5 hours. Further analysis, particularly of the automatic snow sampler data, will be necessary to derive some duration statistics for various concentrations.

It is also of interest that, throughout this work, approximately 50% of all samples comprised rimed snow crystals, which implies that on about half of all occasions when snowfall is occurring at the ground there is some level aloft where mixed cloud conditions of supercooled water droplets and ice crystals may be encountered. The significance of such mixed conditions to aircraft icing is currently under investigation.

#### Conclusions

Of the various meteorological parameters normally recorded, visibility provides the most reliable measure of the atmospheric snow mass concentration. The concentration, in  $\text{g/m}^3$ , is given to within a factor of 2 by the relation

$$C = 2100 V^{-1.29}$$

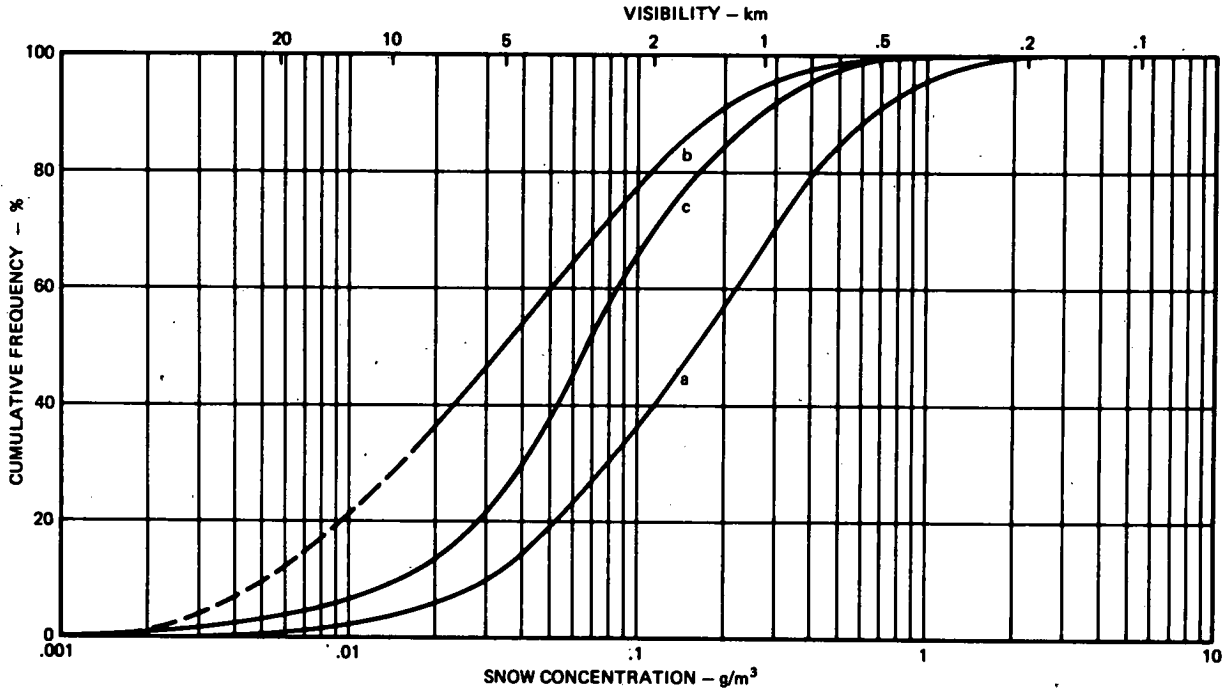
where the visibility,  $V$ , is measured in metres.

A backscatter visibility meter, such as the Videograph, was found to provide an excellent means for estimating the prevailing snow concentration. The output meter of such a device may be scaled in terms of snow concentration to provide a direct readout.

The maximum snow mass concentration so far recorded at Ottawa is  $2.66 \text{ g/m}^3$ , and concentrations in excess of  $1 \text{ g/m}^3$  have been recorded for periods of up to 1.5 hours.

Two probability distribution curves for Ottawa, one derived from actual snow concentration measurements, and the other from visibility records, show some considerable discrepancy; in particular the measured concentration results show a higher probability of higher concentrations. It is expected, though, that the discrepancy will be resolved by forthcoming results from the automatic snow sampler. Should the results from the visibility data be confirmed, then concentration probability data may be derived for any location where climatological records are available.

Figure 8. Cumulative distribution curves of snow concentration for Ottawa: (a) from N.R.C. discrete snow concentration measurements, 1971-77; (b) as derived from diurnal frequencies of reported visibility in combination with snow for the 20-year period 1955-74 at Ottawa International Airport, using the relation  $C = 2100 V^{-1.29}$ ; (c) from 5 snowstorms monitored by N.R.C. automatic snow sampler, 1978.



#### References

1. J. R. Stallabrass. Engine Snow Ingestion in the Bell 206A Jet Ranger Helicopter. NRC, Mech. Eng. Rept. MET-513, 1971.
2. S. R. Brown. Terminal Velocities of Ice Crystals. Colorado State University, Atmospheric Science Paper No. 170, 1970.
3. A. Heymsfield. Ice Crystal Terminal Velocities. J. Atmos. Sci., 29, 1972, pp. 1348-1357.
4. C. Magono. On the Falling Velocity of Solid Precipitation Elements. Sci. Repts. of the Yokohama Nat. Univ., Sec. 1, No. 3, 1954, pp. 33-40.
5. W. D. Harkins and F. E. Brown. The Determination of Surface Tension (Free Surface Energy), and the Weight of Falling Drops: the Surface Tension of Water and Benzene by the Capillary Height Method. J. Amer. Chem. Soc., 41, 1919, pp. 499-524.
6. C. Magono and C. W. Lee. Meteorological Classification of Natural Snow Crystals. Jour. of the Faculty of Science, Hokkaido Univ., Ser. VII (Geophysics), 11, 1966, pp. 321-335.
7. K. Iiou. Light Scattering by Ice Clouds in the Visible and Infrared: a Theoretical Study. J. Atmos. Sci., 29, 1972, pp. 524-526.